Theor Chim Acta (1995) 90: 115–134

Theoretica Chimica Acta

Generalized oscillator strengths of polyatomic molecules
I. H_2O

N. Durante[1], U. T. Lamanna[2], G. P. Arrighini[3], C. Guidotti[3]

[1] Istituto di Chimica Quantistica ed Energetica Molecolare del CNR, Via Risorgimento 35, I-56126 Pisa, Italy

[2] Dipartimento di Chimica dell'Università di Bari, Traversa Re David 200, Campus Universitario, I-70126 Bari, Italy

[3] Dipartimento di Chimica e Chimica Industriale dell'Università di Pisa, Via Risorgimento 35, I-56126 Pisa, Italy
Fax number: + 39-50-918260

Received April 15, 1994/Accepted August 18, 1994

Summary. Generalized oscillator strengths for a number of singlet transitions of the H_2O molecule, evaluated according to the Random Phase Approximation approach, are presented and discussed so as to offer a partial characterization of the Bethe surface of the molecule.

Key words: Generalized oscillator strengths – Bethe surface – Random phase approximation approach – Singlet transitions in water molecule

Introduction

Differential cross sections for inelastic scattering of fast charged particles off atomic and molecular targets are conveniently expressed in terms of the so-called generalized oscillator strengths (GOS) [1–3], first introduced by Bethe [1] over 60 years ago. The role in collision theory of these spectral properties of the target has been particularly advocated by Inokuti [2, 3], who stressed the importance of disposing of the *Bethe surface*, essentially a plot of the density of the generalized oscillator strengths per unit range of transferred energy versus both transferred energy and impulse. Theory demonstrates in fact that this quantity embodies all information about the inelastic scattering of charged particles by an atom or molecule within the 1st Born approximation.

With reference to the case of an electron–molecule collision, let $\boldsymbol{k}_i(\boldsymbol{k}_f)$ denote the impulse of the impinging (emerging) electron, so that $\boldsymbol{q} = \boldsymbol{k}_i - \boldsymbol{k}_f$ is the impulse transferred to the molecule during the collision. The target GOS' considered in the present work are defined as follows (atomic units),

$$F_{n0}(\boldsymbol{q}) = \frac{2E_{n0}}{q^2}\left|\left\langle \psi_n \left| \sum_{j=1}^{N} e^{i\boldsymbol{q}\cdot\boldsymbol{r}_j} \right| \psi_0 \right\rangle\right|^2, \tag{1}$$

E_{n0} is a vertical transition energy from the ground $|\psi_0\rangle$ to the excited electronic state $|\psi_n\rangle$ and $\varepsilon_{n0}(\boldsymbol{q}) = \langle\psi_n|\sum_{j=1}^{N} e^{i\boldsymbol{q}\cdot\boldsymbol{r}_j}|\psi_0\rangle$ the inelastic-scattering form factor [2], a transition property of the target explicitly dependent on the transferred impulse $\boldsymbol{q}$. Since $\langle\psi_n|\sum_{j=1}^{N} e^{i\boldsymbol{q}\cdot\boldsymbol{r}_j}|\psi_0\rangle = \int d\boldsymbol{r}\, e^{i\boldsymbol{q}\cdot\boldsymbol{r}}\rho_{n0}(\boldsymbol{r})$, where $\rho_{n0}(\boldsymbol{r})$ is the diagonal element of the spinless one-body transition density matrix associated with the transition

$|\psi_0\rangle \rightarrow |\psi_n\rangle$ [4], the form factor can be regarded (and possibly evaluated) as the Fourier transform of a proper transition density matrix.

It should be observed that the GOS' defined according to Eq. (1) involve integrations only with respect to electron space and spin coordinates. We are therefore assuming tacitly that a Born–Oppenheimer separation between electronic and nuclear degrees of freedom is a sensible approximation. According to the resulting picture, therefore, both the transition energy E_{n0} and form factor $\varepsilon_{n0}(\boldsymbol{q})$ are vertical quantities specifically evaluated at the equilibrium geometry of the electronic ground state $|\psi_0\rangle$. The assumption of separability between electronic and nuclear motions is ordinarily legitimate for the electronic ground state, but can become questionable for excited states, especially in the cases where near crossings of different molecular terms are involved [2]. Consequences arising from the weakness of the assumption have been reported [5], so one should accept with some caution the general validity of the underlying model.

For the purpose of the present paper it is also convenient to define rotationally averaged GOS values,

$$\langle F_{n0}(q)\rangle_{\text{rot.av.}} = (4\pi)^{-1} \int \mathrm{d}\hat{\Omega}\, F_{n0}(\boldsymbol{q}) \tag{2}$$

with $q = |\boldsymbol{q}|$ and $\hat{\Omega} \equiv (\vartheta, \varphi)$ Euler angles specifying the molecular orientation relative to the vector $\boldsymbol{q}$ assumed along the space-fixed z axis. Inelastic differential cross sections can be (approximately) evaluated under many physically interesting situations starting from rotationally averaged GOS' [6–9]. For a discussion of this subject one is referred to Appendix 1.

From the computational point of view, truly reliable predictions of spectral properties like GOS' require accurate wavefunctions, with many-electron correlation effects taken into account in a balanced way in the couple of quantum states involved in the transition. Even though very noticeable progress toward a solution of the electron correlation problem can nowadays be recognized [10, 11], we are still faced by a very challenging problem, especially exacting in the case of molecular systems. As far as the computational status of transition properties is concerned, the number of really reliable estimates is extremely limited for polyatomic molecules. If we further restrict our attention to the particular case of GOS', to the best of our knowledge only for the first-row hydrides H_2O and NH_3 have accurate values recently been evaluated by *ab initio* CI procedures [12, 13].

By the present paper we propose to start a fairly systematic application of the Random Phase Approximation (RPA) approach [14–18] to the (approximate) prediction of spectral properties of polyatomics, particularly GOS', thus contributing to fill partially a gap of knowledge that is decidedly broad for such class of molecular systems. Starting from popular quantum-chemistry computer programs, RPA offers, as known, a relatively inexpensive and rather practical way for providing estimates, frequently of an acceptable accuracy, for several properties related to excitation processes in which the total spin is conserved [17] (agreement with experiments within 15–20% could be accepted with some confidence). The procedure involves singly and doubly excited electronic configurations, but at the cost of considerably less computational effort than an equivalent CI study would require [19]. At the same time, we offer some comparative results arising from approximations to the RPA approach, in the intent of favouring interpretative speculations.

Without becoming involved in a formal presentation of the RPA approach, that is assumed to be by now widely known, in the next section we present and comment calculated RPA estimates for the GOS' of a number of vertical low-lying electronic transitions in H_2O. Some remarks concerning RPA and its connection to other available approximations are, however, considered relevant to the following discussion. A sketchy review of some salient points is presented in Appendix 2.

Results

There has been a great deal of interest in the past years in studies of the electronic structure of H_2O either from the experimental or the theoretical point of view. In particular, extensive investigations of the molecular photoabsorption, photoionization, photodissociation, photoelectron and electron-impact spectra [20–42] have led to a consistent picture of the markedly Rydberg nature of sequences of excited electronic energy levels of such a molecule, in accordance with a view originally suggested by Mulliken [43].

Setting up a conventional RPA procedure able to describe a number of (vertical) electronic transitions pertaining to the various symmetries A_1, B_1, B_2, A_2 of the H_2O molecule requires that an extended basis set of a_1, b_1, b_2, a_2 HF single particle orbitals be first generated, solutions to the Fock Hamiltonian $\hat{F} = \hat{h} + \sum_{\alpha=1}^{N} (2\hat{J}_\alpha - \hat{K}_\alpha)$, the same for all occupied and unoccupied orbitals of the molecule. As known [23], the unoccupied canonical MO's thus generated do not form an ideally suited set of excited state orbitals for the neutral molecule ($2N$ electrons), but approximate instead those of the negative ion containing $2N + 1$ electrons (see also Appendix 2). They provide, however, an expansion set, in principle complete, a fact that motivates their frequent utilization, for example in the evaluation of electric and magnetic molecular properties by perturbation theory. The required solution of the HF problem has been pursued by us in terms of a many-centre STO basis set expansion. After some laborious experimentation and critical analysis of partial results from a total of 12 extended trial basis sets, we have been led to utilize the following three-center STO basis:

Oxygen nucleus: (DPA) + $3s(1.25167)$ + $3s(0.70733)$ + $3s(0.424)$

+ $4s(0.5305)$ + $4s(0.318)$ + $3p^3(0.95433)$ + $3p^3(0.57267)$

+ $4p^3(0.4295)$ + $3d^5(0.70733)$ + $3d^5(0.424)$

Hydrogen nuclei: (DPA) + $2p^3(0.6625)$

(DPA) is an abridged notation for indicating the STO-basis set employed by Dunning et al. [44] in their near-HF calculations on the electronic ground state of the H_2O molecule. The figures within parentheses represent the exponents of the various Slater orbitals, while the notation $(np)^3$ indicates that all three partners (np_x, np_y, np_z) have been included, with an obvious analogous meaning for $(nd)^5$. The extension of the (DPA) basis so as to include STO's suited for representing low-lying unoccupied orbitals has been carried out according to a procedure suggested in Ref. [45], which specifically involves a scaling of the orbital exponents of STO's playing a major role in the description of the HF ground state electronic density. An evident imbalance of the basis employed with respect to the oxygen center reflects the intention of generating at least the first terms of the Rydberg

Table 1. Some (near) HF property values evaluated for the electronic ground state of H_2O at its experimental geometry: $R_{OH} = 1.810$ a.u., $\langle H\text{–}O\text{–}H = 105°$

	Orbital energy (eV)	Vertical IP (eV) (exptl)[a]
	$-\varepsilon_{1b_1} = 13.9221$	12.61
	$-\varepsilon_{3a_1} = 15.9734$	14.73
$E = -76.0643$ a.u.	$-\varepsilon_{1b_2} = 19.6373$	18.55
$\mu = 1.988$ Debye	$-\varepsilon_{2a_1} = 36.8799$	32.20
	$-\varepsilon_{1a_1} = 559.8117$	539.7

[a] Quoted in Ref. [37]

sequences of levels well documented experimentally for H_2O. In Table 1 we report a few (near) HF properties relative to the electronic ground state of the molecule at its experimental geometry. Among these data, the quantities ε_j represent the orbital energies associated with the five doubly-occupied molecular orbitals, which according to Koopman's theorem should be identified with the successive (vertical) ionization potentials (IP) of the molecule.

The basis set employed originates a totality of 59 unoccupied MO's. A summary of the symmetries and dimensionalities of the vertical electronic excitations obtained from the present RPA calculations is given in Table 2. From the inspection of the table it is seen that the procedure leads to an overall number of 65 excitations from the $X\,^1A_1$ ground state to final states of B_1 symmetry, the analogous numbers for final states belonging to the symmetries B_2, A_1, A_2 being 80, 108 and 42, respectively. The evaluated spectra are found to provide a total of 20 fully bound states with excitation energy $< \mathrm{IP}(1b_1) = 13.92$ eV, so partitioned among the various symmetries: $9\,(^1B_1)$, $5\,(^1A_1)$, $2\,(^1B_2)$, $4\,(^1A_2)$. The remaining 275 vertical excitations fall in spectral regions above the 1st ionization threshold of the molecule. Out of these, 94 correspond to autoionizing final states having excitation energies $< \mathrm{IP}(2a_1) = 36.88$ eV. Even though the L^2-integrable basis functions employed in this paper can lead only to discrete oscillator strengths and transition frequencies, it is known that reliable photoionization profiles can be derived from the computed spectral quantities, for instance by recourse to the Stieltjes–Tchebycheff technique [37, 46].

A number of resonance energies E_{n0} and related (rotationally averaged) dipole oscillator strengths f_{n0} for optically allowed transitions, all starting from the electronic ground state $X\,^1A_1$, are listed in Table 3 in order of increasing excitation within each of the involved symmetries A_1, B_1, B_2. The superscripts (L, V) labeling the oscillator strengths hint at a transition property evaluated according to the "Length" and "Velocity" formulation, respectively [17]. Exact RPA calculations would led to oscillator strength values independent of the formulation adopted (gauge invariance) [47]. It should also be observed that $f_{n0}^{(L)}$ is just the result stemming from Eq. (1) as the transferred impulse $q \to 0$. The data in the table deserve some comments. Excitation energies resulting from our calculations are consistently overestimated in the range 1–1.5 eV compared to the reference values reported. Despite a rather extensive experimentation on the atomic basis and the fact that for each state our calculations have taken into account all particle–hole excitations of the appropriate symmetry, so as to include to a full extent

Table 2. Synoptic table of the numbers and symmetries of excitations between MO's generated by the basis set used in this paper

Orbital	$X\,^1A_1 \rightarrow {}^1B_1$	$X\,^1A_1 \rightarrow {}^1B_2$	$X\,^1A_1 \rightarrow {}^1A_1$	$X\,^1A_1 \rightarrow {}^1A_2$
$1b_1 \rightarrow$	$a_1(27)$	$a_2(5)$	$b_1(11)$	$b_2(16)$
$3a_1 \rightarrow$	$b_1(11)$	$b_2(16)$	$a_1(27)$	$a_2(5)$
$1b_2 \rightarrow$	$a_2(5)$	$a_1(27)$	$b_2(16)$	$b_1(11)$
$2a_1 \rightarrow$	$b_1(11)$	$b_2(16)$	$a_1(27)$	$a_2(5)$
$1a_1 \rightarrow$	$b_1(11)$	$b_2(16)$	$a_1(27)$	$a_2(5)$

inter-channel effects (multichannel RPA, according to a fairly current terminology), we have been unable to go below the values presented, so that we are rather certain that the discrepancy is essentially inherent in the approximation employed. These findings are in accordance with the general experience gained at a computational level with the RPA approach [16–18, 31, 48]. The inclusion of only the $1p$–$1h$ excitations out of the HF ground state, which characterizes such an approximation, is by now known to be usually insufficient to assure truly quantitative accuracy, the important role played, for example, by $2p$–$2h$ components out of a correlated ground state [31, 48, 49] having been totally neglected. The excitation energies shown in the fifth column have been obtained by Yeager et al. [31] in a study designed to clarify some assignments in the electronic spectrum of H_2O through higher quality RPA calculations which include correlation effects to a larger extent than the normal RPA approach does. The scarcity of reliable data for the dipole oscillator strengths allows only a few comments. According to its definition, f_{n0} for a given transition is affected by the error in the excitation energy, with additional effects arising from the approximate evaluation of the transition dipole moment matrix element. On the other hand, RPA is a procedure ideally suited for evaluating directly transition properties [14–18]. The fact that the exact RPA predictions for the dipole oscillator strengths satisfy a number of sum rules, in particular the Thomas–Kuhn–Reiche (TKR) one [14, 17, 47] is an element of consistency in favour of the possible global quality of the RPA oscillator strengths. The overall quality of the RPA observables resulting from our calculations can be judged on the basis of the remarkable invariance of the results with respect to the gauge adopted and the fact that we find $\sum_n f_{n0}^{(L)} \cong \sum_n f_{n0}^{(V)} = 10 + \varepsilon$ with ε small, in very good accordance with the TKR sum rule (see the seventh column of Table 3, where the contributions to the sum rule from the various symmetries involved are separately listed). All calculations suggest also that the transition $4\,{}^1B_2 \leftarrow X\,{}^1A_1$ should correspond to a strongly absorbing band. For some elucidation of the nature of the transition on issue, one is referred to the content of Table 6.

As already remarked, calculations of generalized oscillator strengths are particularly infrequent in the case of polyatomic molecules, even at not very high levels of computational sophistication of the one-body transition density matrix $\rho_{n0}(\boldsymbol{r}, \boldsymbol{r}')$ associated with the excitation process. To the best of our knowledge, for example, we are unaware of GOS calculations at the RPA level for a simple polyatomic molecule like H_2O, all that is available in literature consisting of a couple of papers [12, 22] 20 years apart. Although the first of these papers is still a valuable research contribution despite its being 24 years old, we point at the second paper appeared in 1989 as a true benchmark.

Table 3. RPA vertical excitation energies E_{n0} (eV) and (rotationally averaged) dipole oscillator strengths f_{n0} (a.u.) for the first four excited states belonging to the symmetries A_1, B_1, B_2. All excitations are from the ground state

	E_{n0} (this paper)	E_{n0} (exptl)[a]	E_{n0} (Ref. [31])	$f_{n0}^{(L)}$ (this paper)	$f_{n0}^{(V)}$ (this paper)	$\sum_n f_{n0}^{(L)} \cong \sum_n f_{n0}^{(V)}$ (this paper)	f_{n0}(exptl)	$f_{n0}^{(L)}$ (other calculations)	$f_{n0}^{(V)}$ (other calculations)
	10.919	9.85	9.54	0.073	0.071		0.05[b]	0.06[e]	
A_1	11.459	10.171	9.61	0.030	0.029			0.02[e]	
	12.497	11.057		0.012	0.011				
	12.829	11.432		0.000	0.000	3.32			
	8.675	7.440	7.22	0.046	0.045		0.046[c]; 0.060[d]	0.05[e]; 0.0500[f]	0.0576[f]
B_1	11.176	9.998	9.48	0.012	0.012			0.006[e]	
	11.904	10.640		0.000	0.000				
	12.372	10.990		0.009	0.010	3.39			
	12.401	11.041		0.004	0.003				
B_2	12.638			0.038	0.037				
	14.259			0.007	0.006				
	14.389	13.8		0.166	0.163	3.30			

[a] Ref. [61]
[b] Quoted in Ref. [31]
[c] Harrison AJ, Cederholm BJ, Terwilliger MA (1959) J Chem Phys 30:355
[d] Ref. [32]
[e] Ref. [31]
[f] Ref. [41]

Table 4. (Rotationally averaged) GOS (a.u.) for the transition $1\,^1B_1 \leftarrow X\,^1A_1$ of H_2O as a function of the square transferred impulse q^2(a.u.)

q^2	RPA (present work)	Extended CI[a]	Exptl.[b]
0.030	0.0422	0.0515	0.0527
0.045	0.0402	0.0485	0.0472
0.102	0.0333	0.0390	0.0415
0.144	0.0290	0.0333	0.0315
0.204	0.0237	0.0267	0.0270
0.402	0.0120	0.0134	0.0135
0.900	0.00164	0.00223	0.00219
1.871	0.000512	0.00004	0.00116
3.190	0.00154	0.000699	0.00209
4.402	0.00161	0.00068	0.00216

[a] Ref. [12]
[b] Refs. [32], [33]

In Table 4 our RPA GOS values for the $1^1B_1 \leftarrow X\,^1A_1$ transition in H_2O as a function of the square transferred impulse q^2 are compared with data from both the accurate CI calculation reported in Ref. [12] and experiments. A fairly encouraging agreement over the whole q^2 range is immediately seen, a result that supports further the excellent agreement found for the dipole oscillator strength (Table 3). One observes that our RPA estimates for the case in question decrease, at high q^2 values, more slowly than the CI predictions do, the experiments being for $q^2 > 1.8$ a.u. in seemingly better agreement with the less accurate estimates. Such behaviour, however, should not be emphasized more than so much, considering among other things that inelastic electron collisions in the large q momentum transfer range are insufficiently described by simple recourse to 1st Born approximation, particularly because of the prominence of effects associated with the coupling to the elastic scattering channel arising from the 2nd Born term [50–54]. In addition to this important remark, the GOS' behaviour referred to above could also reflect to some extent the simplified way of obtaining the rotational average adopted in Ref. [12] for generating the quantities $\langle F_{n0}(q)\rangle_{\text{rot.av.}}$ collected in Table 4. We have preferred to resort to an accurate, even though admittedly expensive, averaging procedure based on the integration by double quadrature of GOS' computed at the 16×16 Gaussian points of a square grid of Euler angles (ϑ_i, φ_i), for any $|\boldsymbol{q}|$. The insufficient quality of the basis set employed is a third element to be considered as the transferred impulse increases more and more, as will be argued shortly.

In Table 5 we report (rotationally averaged) RPA GOS' at several values of the transferred impulse q, for a number of vertical transitions to electronic states pertaining to the molecular symmetries $^1A_1$, $^1B_1$, $^1B_2$, $^1A_2$. In all the cases the initial electronic state is the ground state X^1A_1, with the vertical transition taken at the equilibrium geometry of the latter. The behaviour shown by the various GOS' at small q values is different according to whether the transition considered is optically allowed or forbidden. Optically allowed transitions in the electric dipole approximation are usually associated with GOS' decreasing from their maximum

Table 5. (Rotationally averaged) RPA GOS (a.u.) as a function of the transferred impulse q (a.u.) for a number of electronic vertical transitions in H_2O all starting from the ground state $X\,^1A_1$

q	$1\,^1A_1$	$2\,^1A_1$	$3\,^1A_1$	$1\,^1B_1$	$2\,^1B_1$	$3\,^1B_1$	$1\,^1B_2$	$2\,^1B_2$	$3\,^1B_2$	$1\,^1A_2$	$2\,^1A_2$	$3\,^1A_2$
0.1	0.707(−1)	0.297(−1)	0.119(−1)	0.450(−1)	0.113(−1)	0.770(−5)	0.401(−2)	0.377(−1)	0.698(−2)	0.217(−3)	0.790(−5)	0.208(−4)
0.2	0.655(−1)	0.293(−1)	0.105(−1)	0.408(−1)	0.104(−1)	0.329(−4)	0.339(−2)	0.356(−1)	0.626(−2)	0.787(−3)	0.273(−4)	0.906(−4)
0.4	0.481(−1)	0.264(−1)	0.648(−2)	0.275(−1)	0.756(−2)	0.153(−3)	0.192(−2)	0.284(−1)	0.439(−2)	0.214(−2)	0.984(−4)	0.353(−3)
0.6	0.285(−1)	0.202(−1)	0.300(−2)	0.139(−1)	0.449(−2)	0.284(−3)	0.103(−2)	0.194(−1)	0.294(−2)	0.260(−2)	0.288(−3)	0.570(−3)
0.8	0.134(−1)	0.127(−1)	0.116(−2)	0.497(−2)	0.212(−2)	0.268(−3)	0.738(−3)	0.114(−1)	0.217(−2)	0.200(−2)	0.369(−3)	0.548(−3)
1.0	0.480(−2)	0.666(−2)	0.451(−3)	0.101(−2)	0.764(−3)	0.178(−3)	0.583(−3)	0.577(−2)	0.173(−2)	0.112(−2)	0.445(−3)	0.338(−3)
1.2	0.129(−2)	0.310(−2)	0.206(−3)	0.189(−3)	0.201(−3)	0.181(−3)	0.420(−3)	0.256(−2)	0.142(−2)	0.523(−3)	0.443(−3)	0.134(−3)
1.4	0.493(−3)	0.142(−2)	0.110(−3)	0.609(−3)	0.714(−4)	0.281(−3)	0.281(−3)	0.108(−2)	0.117(−2)	0.315(−3)	0.397(−3)	0.270(−4)
1.6	0.687(−3)	0.758(−3)	0.357(−4)	0.120(−2)	0.107(−3)	0.396(−3)	0.190(−3)	0.569(−3)	0.940(−3)	0.356(−3)	0.343(−3)	0.172(−5)
1.8	0.102(−2)	0.519(−3)	0.412(−4)	0.156(−2)	0.173(−3)	0.465(−3)	0.142(−3)	0.505(−3)	0.746(−3)	0.483(−3)	0.294(−3)	0.166(−4)
2.0	0.120(−2)	0.424(−3)	0.275(−4)	0.164(−2)	0.219(−3)	0.475(−3)	0.119(−3)	0.576(−3)	0.584(−3)	0.596(−3)	0.253(−3)	0.412(−4)
2.4	0.110(−2)	0.311(−3)	0.141(−4)	0.133(−2)	0.231(−3)	0.380(−3)	0.950(−4)	0.656(−3)	0.343(−3)	0.662(−3)	0.188(−3)	0.717(−4)
3.0	0.604(−3)	0.170(−3)	0.647(−5)	0.662(−3)	0.156(−3)	0.190(−3)	0.608(−4)	0.457(−3)	0.141(−3)	0.490(−3)	0.113(−3)	0.647(−4)
4.0	0.160(−3)	0.506(−4)	0.192(−5)	0.149(−3)	0.541(−4)	0.420(−4)	0.191(−4)	0.149(−3)	0.278(−4)	0.186(−3)	0.399(−4)	0.270(−4)

value at $q = 0$, with an entirely different behaviour in the optically forbidden cases, where GOS' at $q = 0$ must vanish. Exceptions to the behaviour just described of the optically allowed transitions have been found in our calculations, mainly in the case of higher excitations. Evidence for such occurrences is for example offered by the $3\ ^1B_1 \leftarrow X\ ^1A_1$ GOS' behaviour.

In analogy to the dipole oscillator strengths, a complete set of exact GOS' satisfies a series of sum rules [1, 2]. Out of these, the Bethe sum rule $S(q) \equiv \sum_n F_{n0}(q) = N$ generalizes to the case of $q \neq 0$ the TKR sum rule, independently of the value of the transferred impulse q. Even (exact) RPA GOS' verify the sum rule. The behaviour of $S(q)$ according to our computations is shown in Fig. 1 as a function of q. The various curves refer to RPA calculations (full line) and three different approximations to such approach (SCRPA, TDA, SCTDA) (see Appendix 2). One sees that the Bethe sum rule is very well satisfied by our RPA spectral data up to $q \cong 0.5$ a.u., deviations from $N = 10$ remaining within 10% as q becomes as large as $q \cong 1$ a.u. As q increases beyond such value, however, the finite basis set employed is unable to generate all of the effectively active excitations. Considering that our STO basis set does not include orbitals with azimuthal quantum number $l > 2$ and that higher-order multipole moment contributions to the inelastic-scattering form factor are expected as q increases, the behaviour of $S(q)$ is understandable. The substantial inadequacy (and equivalence) of all the approximations considered as q becomes large is evident from the same figure, a further confirmation of the dominance of basis set effects in such region of values of the transferred impulse, compared to those arising from the neglect of interchannel couplings. It is also interesting to observe in Fig. 1 that the TDA GOS' lead to overestimation of the Bethe sum rule constraint, particularly at relatively small q values.

Some further insight about the role of interchannel coupling effects on calculated GOS values is gained through the inspection of Figs. 2–6, where the GOS behaviour versus the transferred impulse q is displayed for a selection of excitations to a few low-lying final states of different symmetries. In each figure the full RPA GOS curve is compared with others obtained by (in principle) lower-quality

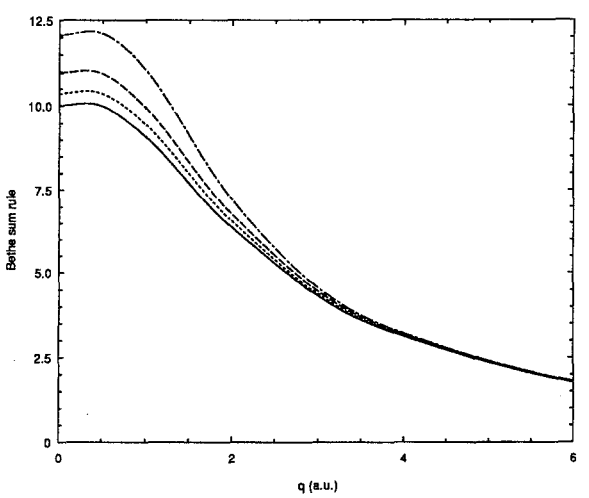

Fig. 1. Behaviour of the quantity $\sum_n F_{n0}(q)$ (Bethe sum rule) as a function of the transferred impulse q. The various curves correspond to RPA (*full line*), TDA (*dash–dotted line*), SCRPA (*dotted line*), SCTA (≡ IVO) (*dashed line*)

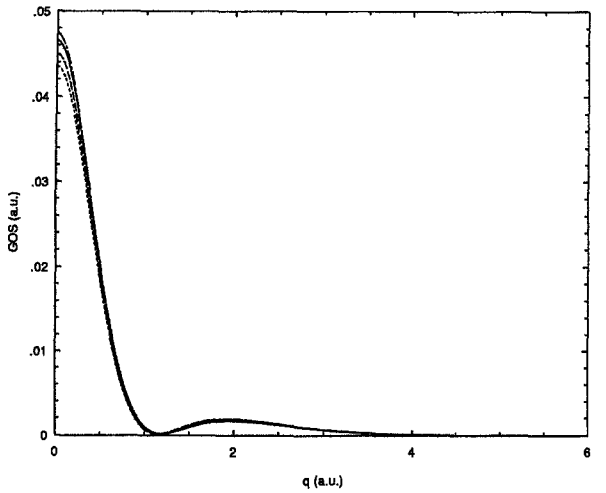

Fig. 2. GOS behaviour for the transition $1\,^1B_1 \leftarrow X\,^1A_1$ as a function of the transferred impulse q. The various curves are drawn according to the caption of Fig. 1

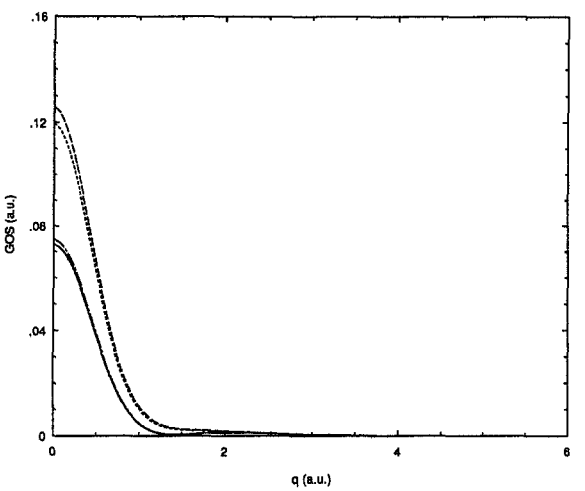

Fig. 3. The same as Fig. 2, for the transition $1\,^1A_1 \leftarrow X\,^1A_1$

treatments, in particular SCRPA and SCTDA, which correspond to separated-channel approximations. As discussed more diffusely in Appendix 2, the SCTDA curves are actually identical to those arising from the so-called improved-virtual-orbital (IVO) spectrum [23]. The main feature emerging from the inspection of the figures is the clear occurrence of multichannel effects, their prominence being particularly remarkable in the case of the final states belonging to the $^1A_1$ and $^1B_2$ symmetries (Figs. 3–5).

To shed further light on the nature of the transitions investigated, we collect in Table 6 some additional qualitative elements, useful to characterize such transitions. In the second column of the table we examine the first four excitations belonging to each of the symmetries $^1A_1$, $^1B_1$, $^1B_2$, $^1A_2$ from the point of view of their more or less marked multichannel character. As immediately seen, the greater number of transitions reported (in particular, the totality of the $^1B_1$ and $^1A_2$ ones) exhibit a weak (W) multichannel nature. Strong (S) or medium (M) interchannel coupling effects are however present in nearly all of the excitations to final states of

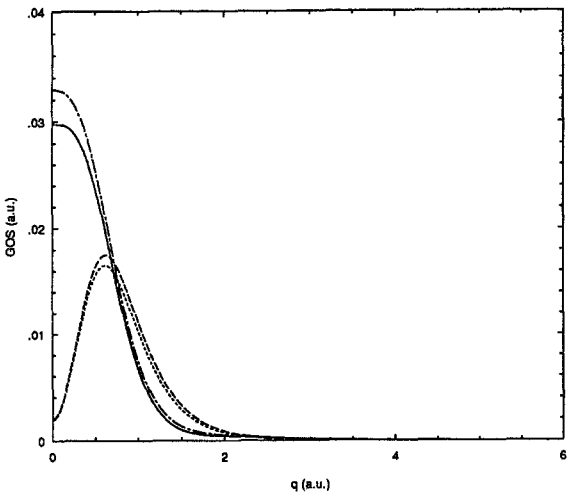

Fig. 4. The same as Fig. 2, for the transition $2\,^1A_1 \leftarrow X\,^1A_1$

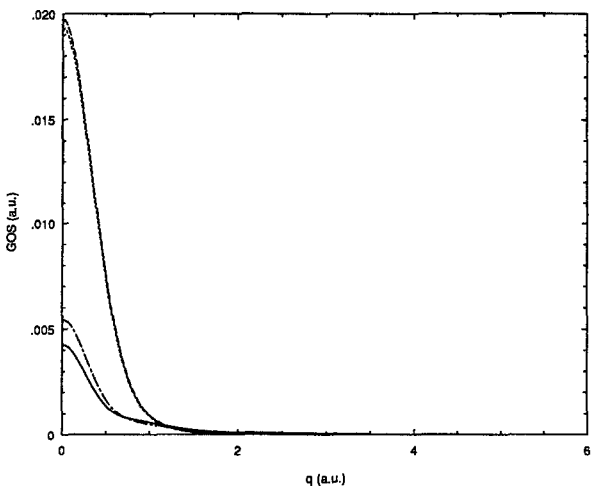

Fig. 5. The same as Fig. 2, for the transition $1\,^1B_2 \leftarrow X\,^1A_1$

$^1A_1$ and $^1B_2$ symmetry, the occupied molecular orbitals mostly involved being in every case the outer ones $1b_1$ and $3a_1$ (our calculations hint at an important role of the orbital $1b_2$ only as far as the $4\,^1B_2 \leftarrow X\,^1A_1$ excitation is concerned). The dominating occupied orbitals in each multichannel excitation (column 3) are given in the order of importance suggested by the relative weight of the amplitudes resulting from our RPA calculations.

In the last column of Table 6 we provide information about the presence of undulations (minima) in the GOS behaviour as q varies. The notation $n(a; b; \ldots)$ provides the number (n) of minima exhibited by the GOS for the transition on issue and the location of such minima, $q = a$, $q = b$, ..., within the range $0 \leqslant q \leqslant 3$ a.u. The possible occurrence of minima can be realized from the simple inspection of the inelastic-scattering form factor, Eq. (1), considering in general the nodal structure of the transition density matrix involved, along with the oscillatory behaviour of the exponential $\exp(i\boldsymbol{q}\cdot\boldsymbol{r})$ [22, 55, 56]. The appearance of the extrema in the GOS curves should be regarded as an interesting and important feature, for it has been suggested that valence and Rydberg transitions could be distinguished

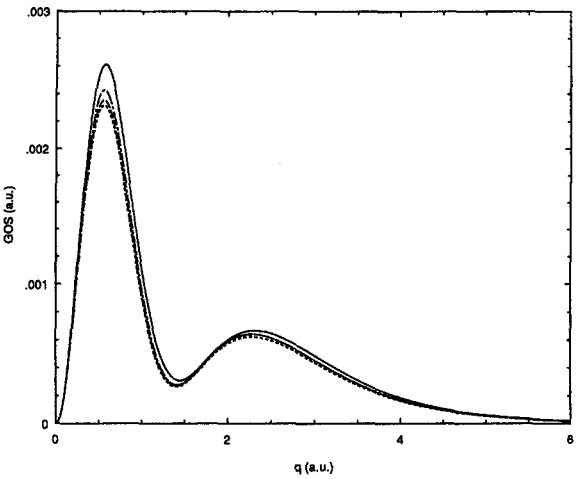

Fig. 6. The same as Fig. 2, for the transition $1\,^1A_2 \leftarrow X\,^1A_1$

even on the basis of the monotonic behaviour or less of the corresponding GOS' as the transferred impulse q is increased [22, 55–60]. Pure Rydberg transitions are intuitively associated with descriptions that should be largely dominated by single orbital effects, as IVO spectra calculations have shown [23, 61, 62]. From our data one actually sees that the presence of minima in the GOS behaviour is not generally related to multichannel effects, considering for example that for the totality of the transitions to final states pertaining to the symmetries $^1B_1$, $^1B_2$, $^1A_2$ both single-channel and multichannel treatments lead to the same kind of behaviour and to essentially identical minima locations. On the other hand, multichannel effects are evident in the case of $^1A_1$ final states. Figures 2–6 allow to obtain a further, clear view of these various behaviours, besides allowing an appreciation of the role of additional multichannel effects, for example in reducing noticeably the $1\,^1B_2 \leftarrow X\,^1A_1$ GOS value at small q. A particularly marked difference between multichannel and single-channel predictions is evident in the case of the $2\,^1A_1 \leftarrow X\,^1A_1$ transition (see Fig. 4), where one notes that the maximum at $q \cong 0.6$ a.u. predicted by single-channel treatments becomes sucked back to $q = 0$ due to multichannel effects, with consequent disappearance of the (spurious) minimum there located. Strong GOS reduction and appearance of slight undulations with a shallow minimum at $q \cong 1.8$ a.u. are noteworthy in the case of the $4\,^1A_1 \leftarrow X\,^1A_1$ transition, still as a consequence of multichannel effects (Fig. 7). In any case, more accurate calculations could be instrumental in sheding light on the nature of the transitions on issue, particularly to exclude the possibility of unphysical RPA artifacts.

As a final comment we recall that in some papers of three of the present authors [7, 63, 64] attempts have been made to assess the role of the electron correlation in the prediction of inelastic scattering cross sections of fast electrons in the case of H_2 molecule. Some evidence was found for a fairly small role of the electron correlation in influencing inelastic-scattering form factors associated with optically allowed transitions. The results of the present paper push in favour of an extension of such behaviour to other molecular systems. Things cannot be, however, so simple in general, considering that X-ray and electron-scattering experiments are admittedly very sensitive probes of the valence-shell electron-correlation effects in the ground electronic states of atoms and molecules. The existence of such connection is at the basis of the relation between electron pair correlation function and

Table 6. Characterization of a number of H_2O molecule (vertical) electronic transitions. S (Strong), M (Medium), W (Weak) is a label denoting the multichannel character of the transition. For the meaning of the last column, one is referred to the text

	Multichannel character	Dominating separated channels	Number of minima in the GOS within the range $0 \leqslant q \leqslant 3$ a.u.			
			RPA	TDA	SCRPA	SCTDA($\equiv$ IVO)
$1\,^1A_1 \leftarrow X\,^1A_1$	S	$3a_1, 1b_1$	1(1.4)	1(1.4)	0	0
$2\,^1A_1 \leftarrow X\,^1A_1$	S	$1b_1, 3a_1$	0	0	1(0.)	1(0.)
$3\,^1A_1 \leftarrow X\,^1A_1$	W	$1b_1$	0	0	0	0
$4\,^1A_1 \leftarrow X\,^1A_1$	M	$1b_1, 3a_1$	2(0.; 1.8)	2(0.; 2.)	1(0.)	1(0.)
$1\,^1B_1 \leftarrow X\,^1A_1$	W	$1b_1$	1(1.2)	1(1.2)	1(1.2)	1(1.2)
$2\,^1B_1 \leftarrow X\,^1A_1$	W	$1b_1$	1(1.4)	1(1.4)	1(1.4)	1(1.4)
$3\,^1B_1 \leftarrow X\,^1A_1$	W	$1b_1$	2($\approx$ 0.; 1.0)	2($\approx$ 0.; 1.0)	2(0.2; 1.0)	2(0.2, 1.0)
$4\,^1B_1 \leftarrow X\,^1A_1$	W	$1b_1$	0	0	0	0
$1\,^1B_2 \leftarrow X\,^1A_1$	M	$1b_1, 3a_1$	0	0	0	0
$2\,^1B_2 \leftarrow X\,^1A_1$	S	$3a_1, 1b_1$	1(1.8)	1(1.8)	1(2.0)	1(2.0)
$3\,^1B_2 \leftarrow X\,^1A_1$	W	$3a_1$	0	0	0	0
$4\,^1B_2 \leftarrow X\,^1A_1$	M	$1b_2, 3a_1$	1(1.6)	1(1.6)	1(1.6)	1(1.6)
$1\,^1A_2 \leftarrow X\,^1A_1$	W	$1b_1$	2(0.; 1.4)	1(0.; 1.4)	2(1.; 1.4)	2(0.; 1.4)
$2\,^1A_2 \leftarrow X\,^1A_1$	W	$1b_1$	1(0.)	1(0.)	1(0.)	1(0.)
$3\,^1A_2 \leftarrow X\,^1A_1$	W	$1b_1$	2(0.; 1.6)	2(0.; 1.6)	2(0.; 1.6)	2(0.; 1.6)
$4\,^1A_2 \leftarrow X\,^1A_1$	W	$1b_1$	1(0.)	1(0.)	1(0.)	1(0.)

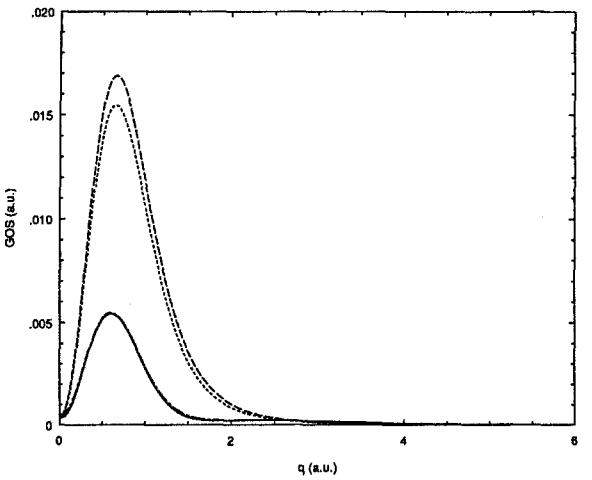

Fig. 7. The same as Fig. 2, for the transition $4\,^1A_1 \leftarrow X\,^1A_1$

experimentally determined GOS', which therefore, taken as a whole, are to be regarded as generally correlation-sensitive properties [65, 66]. Electron correlation effects are in particular expected to play a prominent role in determining such subtle details as the exact location of (shallow) minima in the case of GOS' exhibiting undulations and whether the small GOS minima actually vanish there [12]. Despite these latter observations, RPA is confirmed by the present study as a rather economical and reasonably reliable procedure for exploring in a unique step a sizable portion of the Bethe surface of small polyatomic molecules. The approach appears superior to alternative single-channel treatments in principle adoptable, considering that interchannel couplings leading to collective effects are generally not negligible. One of the main motivations for using RPA today lies probably in its extendibility to fairly large molecular systems, where the application of sophisticated and accurate computational methods is not shortly forseeable. From this standpoint, program packages involving many-centre STO basis sets have been traditionally regarded as a drawback in view of their applicability to significantly large-size molecules, even though such a sentence is becoming not generally shared in a perspective of future trends [67, 68]. Without entering into this hardly explorable domain of possibilities, there is still much room, in our opinion, for significant investigations of the behaviour of small- and medium-size molecular systems in terms of STO's.

Appendix 1

Effects associated with the vibrational and rotational motions of the molecule do not enter into Eq. (1), even if a not ignorable role of nuclear dynamics on the scattering cross sections is expected on general grounds. Although in the present paper we shall not be concerned with the obtainement of the latter observables, some remarks on the matter are in order.

The description of a given molecular electronic transition, in particular one caused by electronic impact, should be regarded as maximally detailed when full information is provided on the ensemble of the individual transitions between all the significantly coupled ro-vibrational states pertaining one to the final and one to

the initial electronic level, respectively. Assuming to a good approximation separability among electronic, vibrational and rotational degrees of freedom, for a collision between an electron and a general polyatomic molecule such information is collected in the matrix elements $\varepsilon(n,\{v'\},J',K',M'\leftarrow 0,\{v''\},J'',K'',M'';q)\equiv\langle\{v'\}J'K'M'|\varepsilon_{n0}(\boldsymbol{q};\{\boldsymbol{R}\})|\{v''\}J''K''M''\rangle$ which generalize the inelastic scattering form factor ε_{n0} appearing in Eq. (1). Clearly $\{v'\}, J', K', M'(\{v''\}, J'', K'', M'')$ are final (initial) vibrational and rotational quantum numbers. It is evident that the calculation of detailed state-to-state form factors requires in principle the electronic quantities $\varepsilon_{n0}(\boldsymbol{q};\{\boldsymbol{R}\})$ to be known at many nuclear configurations $\{\boldsymbol{R}\}$, quite beyond the simplified treatment of the present paper where the GOS' are, according to Eq. (1), vertical properties evaluated at the equilibrium geometry $\{\boldsymbol{R}_0\}$ of the electronic ground state $|\Psi_0\rangle$. While $|\varepsilon(n,\{v'\},J',K',M'\leftarrow 0,\{v''\},J'',K'',M'';q)|^2$ provides one with the most precise description of the electronic transition under study, such a level of detail is in most cases excessive, because rotational levels are usually unresolved in current experiments and can be treated as effectively degenerate. This situation is changing, however, because of the advent of new experimental techniques (zero-kinetic-energy photoelectron spectroscopy, resonance enhanced multiphoton ionization coupled with high-resolution photoelectron spectroscopy, etc.) that allow rotational resolution of molecular photoelectron spectra [69–72]. If we sum $|\varepsilon(n,\{v'\},J',K',M'\leftarrow 0,\{v''\}J'',K'',M'';q)|^2$ over all final rotational quantum numbers (J', K', M') and perform a statistical-mechanical average with respect to the appreciably populated initial rotational states (quantum numbers J'', K'', M''), the resulting quantity is a squared form factor $|\varepsilon_{n0}(\{v'\}\leftarrow\{v''\};q)|^2$ for the transition from the vibrational level $\{v''\}$ in the initial electronic level to the vibrational level $\{v'\}$ belonging to the final electronic level [2]. After neglecting the slight dependence of the modulus q of the transferred impulse on the rotational quantum numbers and exploiting the completeness property of the rotational states one is led by comparison to conclude that $|\varepsilon_{n0}(\{v'\}\leftarrow\{v''\};q)|^2$ is just the same result one would deduce according to the classical method of averaging rotational motions [2, 6–9]. A further simplification follows in the cases where we may assume that the electronic form factor $\varepsilon_{n0}(\boldsymbol{q};\{\boldsymbol{R}\})$ is a slowly varying function of the nuclear geometry coordinates $\{\boldsymbol{R}\}$. $\varepsilon_{n0}(\boldsymbol{q};\{\boldsymbol{R}\})$ can then be replaced by its value at a representative configuration, reasonably $\{\boldsymbol{R}_0\}$ if $\{v''\}$ is the ground vibrational level. In such a case we are left with the result

$$|\varepsilon_{n0}(\{v'\}\leftarrow\{v''=0\};q)|^2=\frac{1}{8\pi^2}\int d\hat{\Omega}|\varepsilon_{n0}(\boldsymbol{q};\{\boldsymbol{R}_0\})|^2\prod_i|\langle v_i'|v_i''=0\rangle|^2$$

the rotational average being neatly factorized out with respect to the vibrational effects, taken into account by the traditional Franck–Condon factors $|\langle v_i'|v_i''=0\rangle|^2$.

The rotationally averaged GOS' defined in Eq. (2) and calculated by us in the present paper should therefore be regarded in the light of these considerations. It is also important to stress that most of the current applications are being based on the acceptance of the approximations illustrated above.

An approximate procedure analogous to that just described can also be developed by working with ro-vibrational states (i.e. without any assumption about the separability of vibrational and rotational motions) and invoking their completeness property. The only requirements are that the incident electron energy be high enough to guarantee the excitation of a practically complete set of these states and that the energy resolution of the experiment is such to permit these states to be included in the spectral line observed. If this is the case, one is led to consider

as relevant quantity a cumulative inelastic differential cross section proportional to $\langle|\varepsilon_{n0}(\boldsymbol{q};\{\boldsymbol{R}\})|\rangle_{\text{st.av.}}$, where $\langle\cdots\rangle_{\text{st.av.}}$ denotes a statistical-mechanical average with respect to populated ro-vibrational states pertaining to the initial electronic level of the molecule. The additional assumption of separability between vibrational and rotational motions allows also in this alternative treatment to reduce the rotational average to a classical one with respect to Euler angles. One should note that at no moment do Franck–Condon factors enter, only a vibrational average in the electronic ground level being required. Franck–Condon factors may however be required to discuss intensities of vibrational features if the vibrational structure of the observed spectral line is resolved.

Appendix 2

The Random Phase Approximation (RPA) is most easily derived by the equations-of-motions method [14, 15], solving for the operator $\hat{O}^+(E)$ that generates an excited state $|E\rangle$ of the Hamiltonian operator $\hat{H}$ from the ground state $|E_g\rangle$

$$\hat{O}^+(E)|E_g\rangle = |E\rangle \tag{A2.1}$$

in such a way to satisfy the Schrödinger equation

$$[\hat{H}, \hat{O}^+(E)]|E_g\rangle = \Delta E|E\rangle \tag{A2.2}$$

with $\Delta E = E - E_g$, excitation energy.

In RPA the operator $\hat{O}^+(E)$ is restricted to the following simple form,

$$\hat{O}^+_{\text{RPA}}(E) = \sum_{m\alpha} [X_{m\alpha}(E)\hat{D}^+_{m\alpha} - Y_{m\alpha}(E)\hat{D}_{m\alpha}]$$

$$\hat{D}^+_{m\alpha} = \hat{a}^+_m \hat{a}_\alpha \tag{A.2.3}$$

where $\hat{a}^+$ and $\hat{a}$ are second-quantized creation and annihilation operators, the subscripts m, α referring to HF particle and hole states, respectively, including the spin functions.

The working RPA equations which stem from Eqs. (A2.1)–(A2.3), according to a procedure extensively discussed in the literature, are usually expressed in the matrix form

$$\begin{pmatrix} \boldsymbol{A} & \boldsymbol{B} \\ -\boldsymbol{B} & -\boldsymbol{A} \end{pmatrix} \begin{pmatrix} \boldsymbol{X} \\ \boldsymbol{Y} \end{pmatrix} = \Delta E \begin{pmatrix} \boldsymbol{X} \\ \boldsymbol{Y} \end{pmatrix}. \tag{A2.4}$$

Any RPA eigenvector involves hole–particle $X_{m\alpha}$ and particle–hole $Y_{m\alpha}$ amplitudes, collected globally in $\boldsymbol{X}$ and $\boldsymbol{Y}$, respectively.

The matrices $\boldsymbol{A}$ and $\boldsymbol{B}$ have elements [71]

$$\boldsymbol{A}_{m\alpha,n\beta} = \langle m\alpha|\hat{H} - E_{HF}|HF\rangle,$$

$$\boldsymbol{B}_{m\alpha,n\beta} = \langle m\alpha n\beta|\hat{H}|HF\rangle, \tag{A2.5}$$

$|HF\rangle$ being the HF approximation to the electronic ground state $|E_g\rangle$ and $E_{HF} = \langle HF|\hat{H}|HF\rangle$. $|m\alpha\rangle \equiv \hat{D}^+_{m\alpha}|HF\rangle$ is a singly excited determinant and $|m\alpha n\beta\rangle \equiv \hat{D}^+_{m\alpha}\hat{D}^+_{n\beta}|HF\rangle$ a doubly excited one.

If the matrix $\boldsymbol{B}$ is neglected, only the sum over $\hat{D}^+_{m\alpha}$ contributes to the excitation operator in Eq. (A2.3), so that the excitation energies ΔE are equivalent to those

obtained by diagonalizing the Hamiltonian matrix in a Hilbert space spanned only by singly excited configurations (Tamm–Dancoff approximation, TDA). The presence of doubly excited states through the matrix $\boldsymbol{B}$ assures that ground state correlation effects are taken into account to some extent.

For the singlet coupling case in which we are interested, the matrix elements of Eq. (A2.5) can be expressed in the form

$$A_{m\alpha,n\beta} = (\varepsilon_m - \varepsilon_\alpha)\,\delta_{\alpha\beta}\delta_{mn} + 2V_{\alpha nm\beta} - V_{\alpha n\beta m}, \qquad B_{m\alpha,n\beta} = 2V_{\alpha\beta mn} - V_{\alpha\beta nm}, \tag{A2.6}$$

the orbital subscripts from now on referring only to the spatial component. In the above equations, $\varepsilon_m(\varepsilon_\alpha)$ denotes the closed-shell HF orbital energy of the particle (hole) state, while the two electron repulsion integrals are defined as follows:

$$V_{ijkl} = \int \mathrm{d}\boldsymbol{r}_1\,\mathrm{d}\boldsymbol{r}_2\, r_{12}^{-1}\,\phi_i^*(\boldsymbol{r}_1)\,\phi_j^*(\boldsymbol{r}_2)\,\phi_k(\boldsymbol{r}_1)\,\phi_l(\boldsymbol{r}_2). \tag{A2.7}$$

Some further remarks are in order at this point. First, the (pseudo) spectra arising from both the RPA and TDA procedures fully carried out cannot be rigorously associated with single discrete configurational excitations, because a given mode receives contributions from all hole–particle and particle–hole excitations (only hole–particle excitations contribute obviously to a TDA mode). One can also speak rightfully of "multichannel" theories, due to the presence of coupling among excitations starting from the various occupied orbitals $\phi_\alpha(\boldsymbol{r})$. Second, the fulfilment of sum rules is only a prerogative of the exact RPA procedure [14, 17, 47, 74], that becomes usually broken (also badly) when introducing approximations to the full approach.

Despite the latter remark, it is both interesting and useful to consider the effect of neglecting any coupling between "channels". To investigate such a point, let us write down the RPA equations for the eigenvector components $\{X_{m\alpha}, Y_{m\alpha}\}$ which follow from Eq. (A2.4) after neglecting all the coupling terms with components $\beta \neq \alpha$. Taking into account the results of Eq. (A2.6) we obtain

$$\begin{aligned}
&[\varepsilon_m - (\varepsilon_\alpha + \Delta E)]\,X_{m\alpha} + \sum_n (2V_{\alpha nm\alpha} - V_{\alpha n\alpha m})\,X_{n\alpha} + \sum_n (2V_{\alpha\alpha mn} - V_{\alpha\alpha nm})\,Y_{n\alpha} = 0,\\
&[\varepsilon_m - (\varepsilon_\alpha - \Delta E)]\,Y_{m\alpha} + \sum_n (2V_{\alpha nm\alpha} - V_{\alpha n\alpha m})\,Y_{n\alpha} + \sum_n (2V_{\alpha\alpha mn} - V_{\alpha\alpha nm})\,X_{n\alpha} = 0.
\end{aligned} \tag{A2.8}$$

If we introduce spatial amplitudes $\{X_\alpha(\boldsymbol{r}), Y_\alpha(\boldsymbol{r})\}$ related to the RPA eigenvector by

$$X_\alpha(\boldsymbol{r}) = \sum_m \phi_m(\boldsymbol{r})\,X_{m\alpha}, \qquad Y_\alpha(\boldsymbol{r}) = \sum_m \phi_m(\boldsymbol{r})\,Y_{m\alpha} \tag{A2.9}$$

and assume that the HF particle states $\{\phi_m\}$ constitute a complete set of real orbitals, after some manipulations we are led to the following coupled equation set for the separated channel RPA (SCRPA) amplitudes $X_\alpha(\boldsymbol{r}), Y_\alpha(\boldsymbol{r})$ [75]

$$\begin{aligned}
&[\hat{F} - (\varepsilon_\alpha + \Delta E)]\,X_\alpha + [2\hat{K}_\alpha - \hat{J}_\alpha]\,X_\alpha + \hat{K}_\alpha Y_\alpha = 0,\\
&[\hat{F} - (\varepsilon_\alpha - \Delta E)]\,Y_\alpha + [2\hat{K}_\alpha - \hat{J}_\alpha]\,Y_\alpha + \hat{K}_\alpha X_\alpha = 0.
\end{aligned} \tag{A2.10}$$

Here $\hat{F}$ is the standard (closed-shell) one-electron Fock operator,

$$\hat{F} \equiv -\frac{1}{2}\nabla^2 + V_{\text{nuc}} + \sum_{\beta}(2\hat{J}_\beta - \hat{K}_\beta) \tag{A2.11}$$

with V_{nuc} the nuclear attractive potential and $\hat{J}_\beta, \hat{K}_\beta$ the usual Coulomb and exchange operators.

It is immediate to put the above equations in the equivalent form

$$\left[-\frac{1}{2}\nabla^2 + V_{\text{nuc}} + \sum_{\beta\neq\alpha}(2\hat{J}_\beta - \hat{K}_\beta) + \hat{J}_\alpha + \hat{K}_\alpha\right] X_\alpha + \hat{K}_\alpha Y_\alpha = (\varepsilon_\alpha + \Delta E)X_\alpha,$$

$$\left[-\frac{1}{2}\nabla^2 + V_{\text{nuc}} + \sum_{\beta\neq\alpha}(2\hat{J}_\beta - \hat{K}_\beta) + \hat{J}_\alpha + \hat{K}_\alpha\right] Y_\alpha + \hat{K}_\alpha X_\alpha = (\varepsilon_\alpha - \Delta E)Y_\alpha. \tag{A2.12}$$

The operator

$$\hat{h}^{\alpha}_{\text{IVO}} \equiv -\frac{1}{2}\nabla^2 + V_{\text{nuc}} + \sum_{\beta\neq\alpha}(2\hat{J}_\beta - \hat{K}_\beta) + \hat{J}_\alpha + \hat{K}_\alpha = \hat{F} - \hat{J}_\alpha + 2\hat{K}_\alpha, \tag{A2.13}$$

is recognized as the familiar one-electron improved virtual orbital (IVO) Hamiltonian, first put forward by Hunt and Goddard [23]. It should be regarded as a modified HF Hamiltonian, with self-Coulomb and exchange removed, able to lead to particle states which are variationally correct approximations to the molecule excited state orbitals (for an unrelaxed core). Equivalently, the virtual orbitals generated by $\hat{h}^{\alpha}_{\text{IVO}}$ are physically meaningful particle states for the neutral molecule, because they stem from adopting, in lieu of the familiar HF potential $\hat{V}_N = \sum_\beta (2\hat{J}_\beta - \hat{K}_\beta)$ (the same for all orbitals) present in the HF operator $\hat{F}$, Eq. (A2.11), a $\hat{V}^{\alpha}_{N-1}$ potential operator representing the proper effect of the other $N-1$ electrons [76–81].

Improved virtual orbitals can be obtained by diagonalizing the matrix $\langle m|\hat{h}^{\alpha}_{\text{NO}}|n\rangle = \varepsilon_m\delta_{mn} + \langle m|2\hat{K}_\alpha - \hat{J}_\alpha|n\rangle$ built in terms of the virtual canonical orbitals arising from the solution of the usual HF problem.

The spectrum generated by $\hat{h}^{\alpha}_{\text{IVO}}$ corresponds to an (infinite) series of Rydberg states accumulating at zero energy [75], the ionization continuum beginning at $\Delta E = -\varepsilon_\alpha$. The interchannel couplings introduced by RPA do not change the ionization thresholds, that remain actually identical to Koopman' theorem IP's.

If the additional approximation of dropping in Eq. (A2.12) the term involving Y_α is legitimate, the resulting eigenvalue problem leads to the IVO (pseudo) spectrum, which is seen to be identical to that arising from the "separated channel" TDA approximation (SCTDA).

Approximate solutions to the RPA problem according to the previous considerations provide a useful zeroth-order spectrum, because the comparison of the latter with that from the full RPA procedure allows one to decide about the possible dominance of excitations from a hole state to a given mode and the role of collective effects related to interchannel couplings.

Acknowledgments. This work has been supported by "Progetto Finalizzato Sistemi Informatici e Calcolo Parallelo" of CNR under grant no. 92.1587.PF69.

References

1. Bethe H (1930) Ann Phys 5:325
2. Inokuti M (1971) Rev Mod Phys 43:297
3. Inokuti M, Itikawa Y, Turner JE (1978) Rev Mod Phys 50:23
4. McWeeny R (1989) Methods of molecular quantum mechanics, 2nd ed. Academic Press, San Diego
5. Mapleton RA (1965) J Chem Phys 42:1846
6. Cartwright DC, Kupperman A (1967) Phys Rev 163:86
7. Arrighini GP, Biondi F, Guidotti C (1980) Mol Phys 41:1501
8. Read FH, Whiterod GL (1963) Proc Phys Soc 82:434
9. Rescigno TN, McCurdy CW, McKoy V, Bender CF (1976) Phys Rev A13:216
10. Wilson S (ed) (1987) Methods in computational chemistry, Vol 1. Plenum, New York
11. Dykstra CE (1988) Ab initio calculation of the structures and properties of molecules. Elsevier, Amsterdam
12. Bhanuprakash K, Chandra P, Chabalowski C, Buenker RJ (1989) Chem Phys 138:215
13. Chantranupong L, Hirsch G, Buenker RJ, Kimura M, Dillon MA (1991) Chem Phys 154:13
14. Rowe DJ (1968) Rev Mod Phys 40:153
15. Shibuya T, McKoy V (1970) Phys Rev A2:2208
16. Herman MF, Freed KF, Yeager DL (1981) Adv Chem Phys XLVIII:1
17. Oddershede J, Jørgensen P, Yeager DL (1984) Comp Phys Rep 2:33
18. Oddershede J (1987) Adv Chem Phys LXIX:201
19. Galasso V (1985) J Chem Phys 82:899
20. Skerbele A, Meyer VD, Lassettre EN (1965) J Chem Phys 43:87
21. Marr GV (1967) Photoionization processes in gases. Academic Press, New York
22. Miller KJ, Mielczarek SR, Krauss M (1969) J Chem Phys 51:26
23. Hunt WJ, Goddard WA (1969) Chem Phys Letters 3:414
24. Turner DW, Baker C, Baker AD, Brundle CR (1970) Molecular photoelectron spectroscopy. Wiley, New York
25. Clayton CR, Segal GA, Taylor HS (1971) J Chem Phys 54:3799
26. Franks F (ed) (1972) Water – A comprehensive treatise, Vol 1. Plenum, New York
27. Trajmar S, Williams W, Kupperman A (1973) J Chem Phys 58:2511
28. Bonham RA, Fink M (1974) High energy electron scattering, ACS monograph 169. Van Nostrand Reinhold, New York
29. Goddard WA, Hunt WJ (1974) Chem Phys Lett 24:464
30. Buenker RJ, Peyerimhoff SD (1974) Chem Phys Lett 29:253
31. Yeager D, McKoy V, Segal GA (1974) J Chem Phys 61:755
32. Lassettre EN, Skerbele A (1974) J Chem Phys 60:2464
33. Klump KN, Lassettre EN (1975) Can J Phys 53:1825
34. Zeiss GD, Meath WJ, MacDonald JCF, Dawson DJ (1977) Radiat Res 70:284
35. Wang H-T, Felps WS, McGlynn SP (1977) J Chem Phys 67:2614
36. Tan KH, Brion CE, Van der Leeuw PE, Van der Wiel MJ (1978) Chem Phys 29:299
37. Cacelli I, Moccia R, Carravetta V (1984) Chem Phys 90:313
38. Moccia R, Rizzo A (1985) J Phys B18:3319
39. Cacelli I, Carravetta V, Moccia R (1986) J Chem Phys 85:7038
40. Geertsen J, Oddershede J, Sabin JR (1986) Phys Rev A34:1104
41. Phillips RA, Buenker RJ (1987) Chem Phys Letters 137:157
42. Cacelli I, Carravetta V, Moccia R, Rizzo A (1988) J Phys Chem 92:979
43. Mulliken RS (1935) J Chem Phys 3:506
44. Dunning TH, Pitzer RM, Aung S (1972) J Chem Phys 57:5044
45. Guidotti C, Lamanna UT, Arrighini GP, Durante N (1992) J Mol Struct (Theochem) 254:77
46. Rescigno TN, Bender CF, McKoy BV, Langhoff PW (1978) J Chem Phys 68:970
47. Harris RA (1969) J Chem Phys 50:3947
48. Rose J, Shibuya T, McKoy V (1973) J Chem Phys 58:74
49. Shibuya T, Rose J, McKoy V (1973) J Chem Phys 58:500
50. Kelsey EJ (1976) Phys Rev A14:56

51. Shakeshaft R (1977) Phys Rev A16:1458
52. Bielschowsky CE, Nascimento MAC, Hollauer E (1992) Phys Rev A45:7942
53. Huo WM (1972) J Chem Phys 57:4800
54. Bonham RA (1974) J Electron Spectr Related Phenomen 3:85
55. Bonham RA (1962) J Chem Phys 36:3260
56. Kim Y-K, Inokuti M, Chamberlain GE, Mielczarek SR (1968) Phys Rev Letters 21:1146
57. Miller KJ (1969) J Chem Phys 51:5235
58. Krauss M, Mielczarek SR (1969) J Chem Phys 51:5241
59. Miller KJ (1971) Intern J Quantum Chem 5S:71
60. Domenicucci AG, Miller KJ (1977) J Chem Phys 66:3927
61. Gürtler P, Saile V, Koch EE (1977) Chem Phys Lett 51:386
62. Williams GRJ, Langhoff PW (1979) Chem Phys Lett 60:201
63. Arringhini GP, Biondi F, Guidotti C, Biagi A, Marinelli F (1980) Chem Phys 52:133
64. Arrighini GP, Guidotti C, Durante N (1990) In: Capitelli M, Bardsley JN (eds) Nonequilibrium processes in partially ionized gases. Plenum, New York
65. Ketkar SN, Bonham RA (1986) Int J Quantum Chem Symp 20:627
66. Barbieri RS, Bonham RA (1991) Phys Rev A44:7361
67. Bouferguene A, Rinaldi D (1994) Int J Quantum Chem 50:21
68. Kutzelnigg W (1988) J Mol Struct (Theochem) 181:33
69. Kuge H-H, Kleinermanns K (1989) J Chem Phys 90:46
70. Tomkyn RG, Wiedmann R, Grant ER, White MG (1991) J Chem Phys 95:7033
71. Lee M-T, Wang K, McKoy V (1992) J Chem Phys 97:3905
72. Wang K, Stephens JA, McKoy V (1993) J Phys Chem 97:9874
73. Ostlund N, Karplus M (1971) Chem Phys Lett 11:450
74. Hansen AE, Bouman TD (1979) Mol Phys 37:1713
75. Yabushita S, McCurdy CW, Rescigno TN (1987) Phys Rev A36:3146
76. Kelly HP (1964) Phys Rev 136:B896
77. Huzinaga S, Arnau C (1970) Phys Rev A1: 1285
78. Huzinaga S, Arnau C (1971) J Chem Phys 54:1948
79. Amusya MY, Cherepkov NA, Chernysheva LV (1971) Sov Phys-JETP 33:90
80. Ficocelli Varracchio E (1984) J Phys B: At Mol Phys 17:L611
81. Harris FE, Monkhorst HJ, Freeman DL (1992) Algebraic and diagrammatic methods in many-fermion theory. Oxford University Press, Oxford